

2017

Validation of Pair-Potential Models for Use in Simulating Titanate Nanostructures

Nicholas Lima Acosta
Lehigh University

Follow this and additional works at: <https://preserve.lehigh.edu/etd>

 Part of the [Mechanical Engineering Commons](#)

Recommended Citation

Acosta, Nicholas Lima, "Validation of Pair-Potential Models for Use in Simulating Titanate Nanostructures" (2017). *Theses and Dissertations*. 2979.
<https://preserve.lehigh.edu/etd/2979>

This Thesis is brought to you for free and open access by Lehigh Preserve. It has been accepted for inclusion in Theses and Dissertations by an authorized administrator of Lehigh Preserve. For more information, please contact preserve@lehigh.edu.

Validation of Pair-Potential Models for Use in Simulating Titanate
Nanostructures

by

Nicholas L. Acosta

A Thesis

Presented to the Graduate and Research Committee

of Lehigh University

in Candidacy for the Degree of

Master of Science

in

Mechanical Engineering

Lehigh University

January 2018

©2018

Nicholas L. Acosta

All Rights Reserved

This thesis is accepted and approved in partial fulfillment of the requirements for the Master of Science.

Date

Edmund Webb III, Advisor

D. Gary Harlow, Chairperson
Department of Mechanical Engineering and Mechanics

Acknowledgements

First, I would like to thank Dr. Edmund Webb III for providing the opportunity to conduct this research for my Master's thesis. Thanks to this opportunity, I have become a well-rounded engineer in getting to understand in more detail the atomistic world around us and how it relates to the macro world. I also have to thank him for his constant support in helping me understand and comprehend the skills that were required of me to understand the subject matter.

I also need to thank Dr. Nipun Goel and Dr. Baiou Shi for their guidance in getting started with and learning the intricacies of LAMMPS and running simulations on Lehigh's HPC clusters at the beginning of my research.

Finally, not enough can be said about the support that I have had from my family and friends in the pursuit of my Master's thesis. I can not be thankful enough for the pushes of motivation and wise-words that were shared along the way.

Contents

Title Page	i
Copyright	i
Approvals	ii
Acknowledgments	iii
Abstract	1
1 Introduction	2
1.1 Research Opportunity	2
1.2 Thesis Objectives	3
1.3 Thesis Structure	4
2 Background	5
2.1 Titanates	5
2.1.1 Rutile	7
2.1.2 Anatase	8
2.2 Molecular Dynamics	10
2.3 Matsui-Akaogi Potential	12
2.3.1 Core-Shell Extension	13
3 Simulations and Discussion	15
3.1 Validating the Model	15
3.1.1 Building a Titanate Bulk	15
3.1.2 Minimizing the Bulk Energy	18
3.1.3 Simulating for Size Effects	21
3.2 Nanowire Simulation	25
4 Future Work	31

List of Tables

2.1	List of basis atom positions in the rutile phase unit cell	8
2.2	List of basis atom positions in the anatase phase unit cell	10
2.3	Energy parameters as defined by MA potential	13
2.4	Core and Shell Charges	14
2.5	Buckingham Potential Parameters	14
3.1	Lattice values for titanate bulk structures	19
3.2	Surface Energies of Slab versus Slab Size	24

List of Figures

2.1	An image of a natural anatase formation[17]	6
2.2	An atomic model of the crystalline rutile phase of TiO_2 [19]	7
2.3	An atomic model of the crystalline rutile phase unit cell[19]	8
2.4	An atomic model of the crystalline anatase phase of TiO_2 [19]	9
2.5	An atomic model of the crystalline anatase phase unit cell[19]	9
2.6	Modeling techniques in relation to length and time scales addressed[21]	11
3.1	Density profile of anatase bulk along the X (a lattice) axis direction. This sample was about 20 Å on edge.	17
3.2	Density profile of anatase bulk along the Z (c lattice) axis direction. This sample was about 20 Å on edge.	17
3.3	Atom positions before and after minimization runs of a 20 Å on edge bulk crystal.	18
3.4	Density profile of anatase bulk along the X (a lattice) axis direction after minimization and shift. This sample was about 20 Å on edge.	20
3.5	Density profile of anatase bulk along the Z (c lattice) axis direction after minimization and shift. This sample was about 20 Å on edge.	21
3.6	Anatase slab with periodicity removed in the X (a lattice) axis direction before and after relaxation. This sample was about 20 Å on edge.	22
3.7	Anatase slab with periodicity removed in the Z (c lattice) axis direction before and after relaxation. This sample was about 20 Å on edge.	22
3.8	Density profile of anatase bulk along the X (a lattice) axis direction after relaxation. This sample was about 20 Å on edge.	23
3.9	Density profile of anatase bulk along the Z (c lattice) axis direction after relaxation. This sample was about 20 Å on edge.	24
3.10	Simulation cell of anatase nanowire at the initial simulation timestep.	25
3.11	Simulation cell of anatase nanowire at the final simulation timestep.	26
3.12	Potential energy of nanowire simulation with respect to time.	28
3.13	Image of simulated anatase nanowire array at the initial simulation timestep. Only the center set of atoms were simulated (inside bounding box), all others are a representation of the nanowires surrounding the center.	28

3.14 Image of simulated anatase nanowire array at the final simulation timestep. Only the center set of atoms were simulated (inside bounding box), all others are a representation of the nanowires surrounding the center.	29
--	----

Abstract

In this thesis, a potential model for simulating titanium oxides (titanates) is studied. Titanium oxides are of importance for their photo-voltaic properties and their ability to be synthesized into nanostructures, such as nanoparticles and nanofibers; the ability to synthesize titanates into such nanostructures can benefit their performance in photovoltaic applications. Thus, the construction of a foundation for future simulation work using a charge transfer enabled potential is of importance. The goal here is to understand if an existing potential model can be applied to any given form of titanium oxide or if there are portions of the potential that lack the ability to simulate specific items that are required to move forward with the simulation of zero dimensional (particles), one dimensional (wires and tubes) and two dimensional (sheets) titanate nanostructures.

Chapter 1

Introduction

1.1 Research Opportunity

As the current technology revolution continues, there is a need to prepare to step away from unsustainable power generation techniques and to grow in the fields of energy generation and storage from renewable and sustainable energies[1]. To accomplish this, new materials and processes must be researched and developed to sustain the growth of the technology[2].

One such class of materials that has been developed due to this recent technological push is one-dimensional (1D) materials[3]. 1D materials are important as they have unique mechanical, electrical, thermal, optical and chemical characteristics. There are several materials that can be made into nanostructures, such as carbon (nanotubes and graphene sheets)[4][5][6], gold (and other metals)[7][8][9], and important semiconductors like gallium nitride[10]. Other materials that are currently being researched are titanium oxides (TiO_2), titanates[11].

Titanates are important as they have well known photo-voltaic and semiconducting properties, and are currently used in dye-sensitized solar cells in a nanoparticle form; however experimental data show that that nanofiber form of titanates have improved photo-voltaic efficiency[12]. Furthermore, current research has reviewed

methods of synthesis and some of the unique properties of the titanate material in a 1D form but have provided little in way of the fundamental knowledge of the relationships between how the material is processed, the structure it undertakes, and the properties that this structure provides.

1.2 Thesis Objectives

The goals of this thesis are focused around the study of a potential atomic model of titanate materials:

- One goal is to evaluate the application of an existing core-shell material interaction model suitable for use in molecular dynamics simulations to the simulation of titanate interactions with lithium.
- A second goal is to apply the core-shell type potential to simulate a titanium nanofiber and evaluate the efficiency of this model for future studies of titanate nanostructures.

As mentioned in the previous section, there have been other investigations using molecular dynamics into titanates and their interactions with other charged, such as lithium ions (Li^+). These studies are of recent publication and still require vetting with respect to the transferability of the model to studying general titanate nanostructures. The first objective of this thesis is to evaluate the model to be used, a modification of the Matsui-Akaogi method of simulating titanium oxides, in which a core-shell model has been adapted to better represent the charge modeling (i.e. polarizability) in a titanate structure.

The second objective is to apply the model to the simulation of a crystalline nanofiber. The focus of this study is to evaluate the suitability of an existing model when applied to nanostructure. Furthermore, it is a related goal of this study to see how the model behaves with free-surfaces in two dimensions and whether such

simulated geometries remain stable.

1.3 Thesis Structure

This thesis will be presented in the following manner. Chapter 2 will discuss the background information relevant to the research conducted, including the structure of titanates, methods for building a model of a structure for computational simulation, and computational methods for simulating the structure. The computational methods for simulation will introduce the concepts of molecular dynamics and the workings of the computational potentials (i.e. the material interatomic models) chosen for the thesis. Chapter 3 will focus on the model when applied to the simulation of a nanostructure to confirm whether the potential chosen is a good candidate to support future research in this area. This chapter will discuss the development of the simulation experiments using the molecular dynamics code LAMMPS and discuss the simulation results. Chapter 4 will present a road map for the future research recommended to follow efforts described in this thesis.

Chapter 2

Background

2.1 Titanates

Titanates are materials built from titanium (Ti) and oxygen (O), often in the chemical stoichiometry TiO_2 . These materials can be found both in nature, such as shown in Figure 2.1 and manufactured in labs; they typically manifest in one of three crystalline forms; rutile, anatase, and brookite. Each of these forms are built of three titanium atoms coordinating with an oxygen atom and six oxygen atoms coordinating with a titanium atom. However, the way in which the atoms are oriented are distorted between the three forms gradually going from rutile to brookite[13].

There are several processes in which these structures can be formed in a laboratory setting. The sol-gel method[14][15], is a common method in which to make ceramics, in which an amount of the material to be synthesized is dispersed in a liquid gel solution. This gel is then cast into a mold of a desired shape to avoid the gel adhering to the mold. Once in the mold, the solution begins to gel; this is the point at which fibers can be pulled or spun. Once the solution goes through three more steps of aging, drying, dehydration, and densification at high temperature, the fibers are prepared. Another hydro-gel synthesis process,



Figure 2.1: An image of a natural anatase formation[17]

patented by Lehigh's Dr. Animesh Kundu, raises a solution of the desired material to an elevated temperature, combined with rapid stirring in a sealed environment; this produces the desired nanofibers described in the preceding chapter[16].

It is worth mentioning however that current applications of titanium oxides are mostly limited to rutile and anatase as these are the more common phase to be synthesized. The remainder of this thesis will then focus on these two titanate phases.

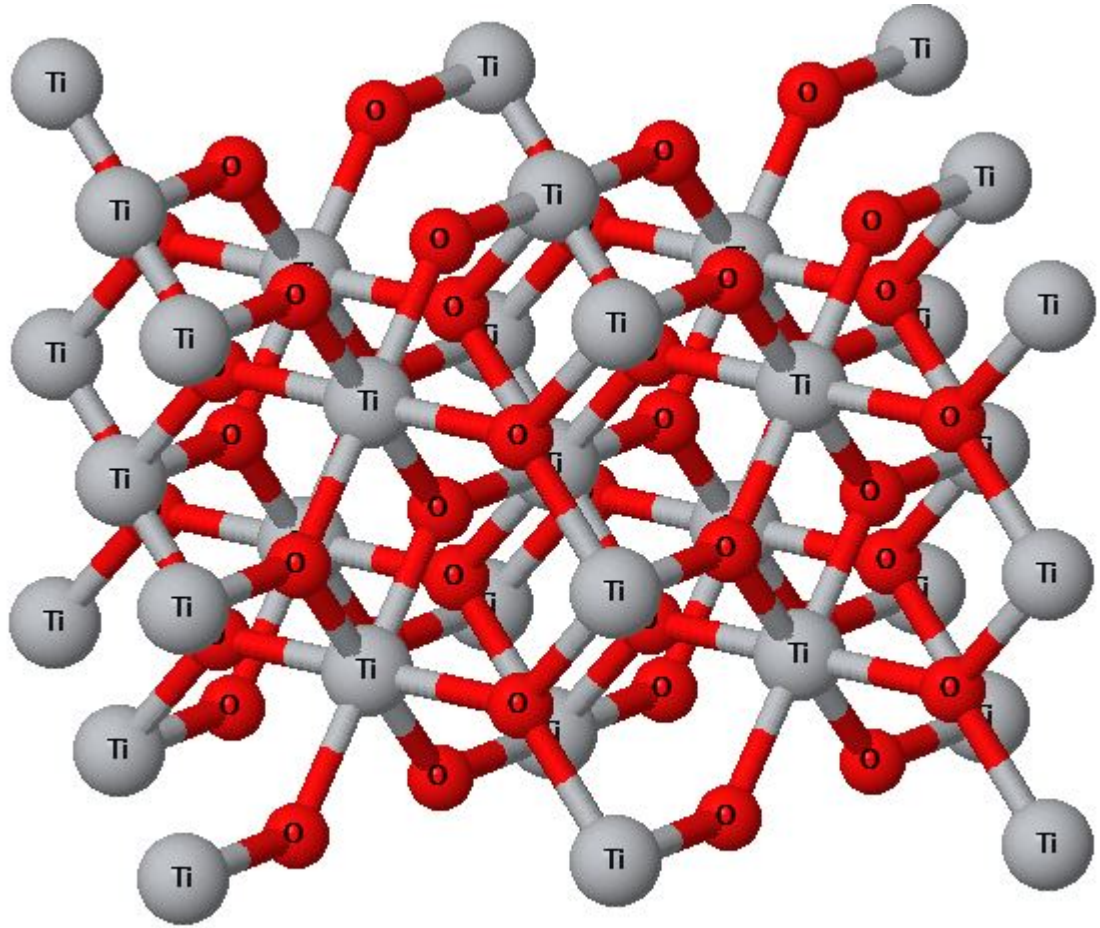


Figure 2.2: An atomic model of the crystalline rutile phase of TiO_2 [19]

2.1.1 Rutile

Rutile is the most stable form of a titanate, having the least distorted of the bonds between titanium and oxygen. Its crystalline structure is considered tetragonal and belongs to the space group $D_{4h}^{14} - P4_2/mnm$. Figure 2.2 shows an atomic model of the rutile crystal structure, which was then used to derive the unit cell in Figure 2.3. The equilibrium in-plane lattice constant is $a = b = 4.584 \text{ \AA}$ and the out-of-plane is $c = 2.953 \text{ \AA}$ [18]. The basis vectors for the atoms are tabulated in Table 2.1.

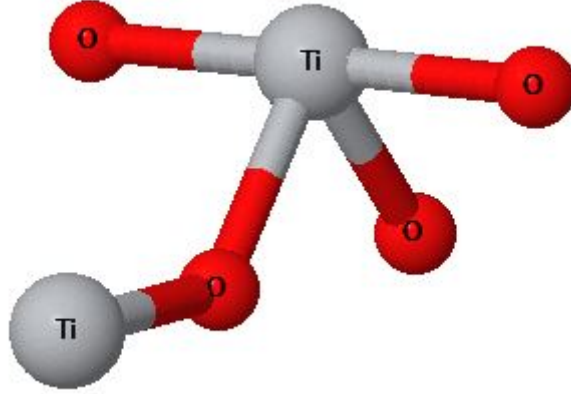


Figure 2.3: An atomic model of the crystalline rutile phase unit cell[19]

Table 2.1: List of basis atom positions in the rutile phase unit cell

Atom	a	b	c
Ti_1	0	0	0
Ti_2	0.5	0.5	0.5
O_1	0.3048	0.3048	0
O_2	0.6952	0.6952	0
O_3	0.8048	0.1952	0.5
O_4	0.1952	0.8048	0.5

2.1.2 Anatase

Anatase is the second most common formation of titanium dioxide in nature. Its crystalline structure is similar to that of rutile; however it is slightly distorted comparatively. It is still considered a tetragonal crystal but belongs to the space group $D_{4h}^{19} - I4_1/amd$. Figure 2.4 shows shows an atomic model of the anatase crystal structure, which like the rutile crystal, was then used to derive the unit cell in Figure 2.5 . The equilibrium in-plane lattice constant is $a = b = 3.733 \text{ \AA}$ and its out-of-plane is $c = 9.370 \text{ \AA}$ [18]. The basis vectors for the atoms are tabulated in Table 2.2.

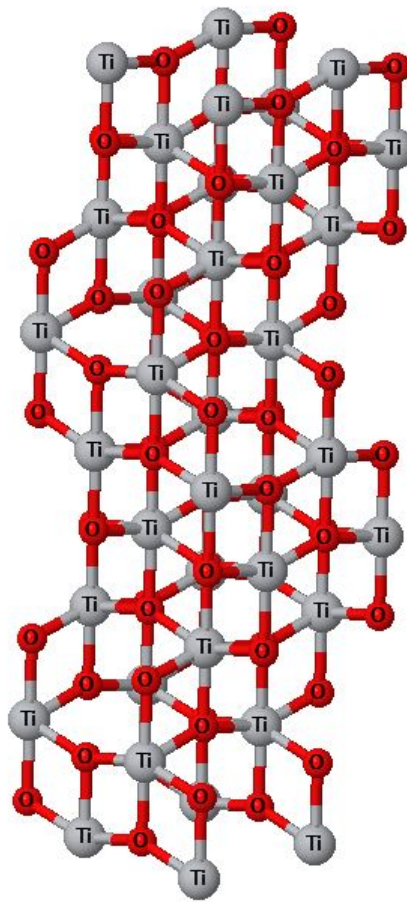


Figure 2.4: An atomic model of the crystalline anatase phase of TiO_2 [19]

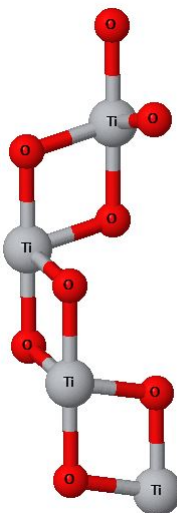


Figure 2.5: An atomic model of the crystalline anatase phase unit cell[19]

Table 2.2: List of basis atom positions in the anatase phase unit cell

Atom	a	b	c
Ti_1	0	0	0
Ti_2	0	0.5	0.25
Ti_3	0.5	0.5	0.5
Ti_4	0.5	0	0.75
O_1	0	0	0.2077
O_2	0	0.5	0.0423
O_3	0.5	0.5	0.2923
O_4	0	0.5	0.4577
O_5	0.5	0	0.5423
O_6	0.5	0.5	0.7077
O_7	0.5	0	0.9577
O_8	0	0	0.7923

2.2 Molecular Dynamics

Molecular dynamics (MD) is the application of statistical mechanics and computer simulation techniques to explore the behavior of atoms and molecules[20]. These simulations can be used in a way similar to physical experimentation, and can be used to study the phenomena occurring at the atomic scale of macro-world problems. To achieve the accuracy required for these simulations to represent the probable outcomes of the physical experiments or processes they are run with small time step increments, in order of pico- to femto- second. This makes MD valuable to link the gap between the expected microscopic behaviors and macroscopic experiments, as shown in Figure 2.6. It also makes MD unsuitable for continuum (macro) scale simulations.

The process in which these simulations are conducted is similar to that of physical experiments. Initially a model must be built to run the simulation

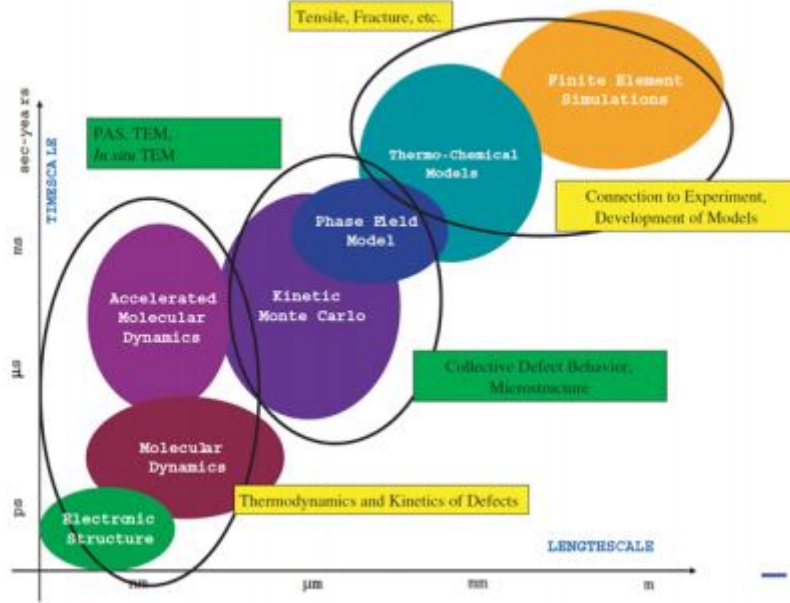


Figure 2.6: Modeling techniques in relation to length and time scales addressed[21]

of. These models can range from a few hundred particles to a couple of billion, depending on what kind of processing power is available to the research scientist[22]. Once a model is constructed, validation of the model is necessary. This often includes running a simulation of the model and checking results against pre-determined values of the properties of the material. An example of this is running a simulation and observing what the average lattice constant of a crystalline material is reported to be at temperature $T=300$ K, this should match up to the known value for the material being simulated. After such validation, the production runs are essentially a set of numerical experiments can be conducted using different calculations on the model to simulate different conditions. However as mentioned previously, due to the limited computing power available to run these simulations, only small pieces of a given problem can be simulated. This gives researchers small bits related to valuable information of a much bigger picture to analyze[23].

For the work in thesis, MD is an appropriate tool to understand the behaviors of the model and how it compares to the real world observed behaviors of the material in a one dimensional and two dimensional form, as nano-fibers of titanium oxides

tend to be in the nanometer scale in diameter. MD will allow the size effects of the interactions between the coulombic charges of the titanium and oxygen ions to be analyzed, as well as any free-surface boundary reconstructions due to the effects of the size or strain imparted by the nano-geometry.

Molecular dynamics is based on the idea that particles, for instance atoms, within a distance of each other will interact and exert a force on each other. In the simplest examples of so-called pair potentials these forces are determined by the distance of separation between two atoms, r ; this separation determines the potential energy through the inter-atomic potential model of the system U which is then related to force using the following equation[24]:

$$F(r) = -\frac{\partial U(r)}{\partial r} \quad (2.1)$$

This equation is applied to all sets of particles within a cutoff range. Therefore, one must be careful as to which pair potential is used in a given simulation as the requirements of a given simulation may not match just any given potential. Common pair potentials are the Lennard-Jones potential[25], Buckingham potential[26], and the Coulombic potential. It is not uncommon to see a combination of potentials to be used as well within a model, as interactions between different type of particles may warrant the use of different potentials.

2.3 Matsui-Akaogi Potential

As mentioned above, the potential used in the model is imperative to success of any MD simulation. Therefore, for this thesis, the chosen potential was an improvement upon an initial simpler potential, the Matsui-Akagoi (MA) potential for titanium oxide polymorphs[27]. Therefore, to gain a better understanding of the groundwork of the potential used in this thesis it is important to discuss the MA potential first.

The MA potential combines several individual potentials to generate its pairwise potential for titanates. It uses a coulombic, dispersion, and a repulsion term with constants that have had quantum corrections applied during optimization of the potential. The potential takes the form:

$$V_{ij} = q_i q_j r_{ij}^{-1} - C_i C_j r_{ij}^{-6} + f(B_i + B_j) * \exp[(A_i + A_j - r_{ij}) / (B_i + B_j)] \quad (2.2)$$

In this form, r_{ij} is the interatomic distance of two atoms, q_i is effective charge, A_i is the repulsive radius, B_i is the softness parameter, and C_i is the van der Waals coefficient, all for an atom i . The quantity f is a set constant of $4.184 \text{ kJ } \text{\AA} \text{ mol}^{-1}$. The effective charge of q_O is equivalent to the $-q_{Ti}/2$. The C_O is taken to be $2916 \text{ \AA}^6 \text{ kJ/mol}$. Along with the remaining parameters defined per atom as shown in Table 2.3. Using these parameters the MA potential proved to be aligned

Table 2.3: Energy parameters as defined by MA potential

Atom	q(e)	A(\AA)	B(\AA)	C(\AA ³ kJ ^{0.5} mol ^{-0.5})
<i>Ti</i>	+2.196	1.1823	0.077	22.5
<i>O</i>	-1.098	1.6339	0.117	54.0

with the observed experimental data of the titanates studied with minor quantum correction, within 2% for simulated runs at 300K and 0 GPa.

2.3.1 Core-Shell Extension

In order to properly describe polarizability present in titanates, it was necessary to advance the potential proposed by Mastui and Akagoi. The reasoning behind this decision was that the MA model was developed for a rigid ion structure, this meant that the results of the pure MA potential would overestimate energies of any reorganization within the simulation model. Put differently, important relaxations of TiO_2 polymorphs are stabilized by polarizability of the material.

Briefly, polarizability refers to the ability of the plus minus charges of the oxygen atom nucleus and electron valance shell, respectively, to exhibit spatial anisotropy, resulting in local dipoles. Therefore, *Kerisit et. al.*[28] developed a model that modified the MA potential to include polarizability effects and thereby better simulate this type of charge behavior. Therefore, this potential uses an additional potential term in which the oxygen atoms are simulated using a core and shell method. The core-shell method breaks an atom down into two parts: the nucleus and the electron cloud, where the cloud is the shell. To do this the potential energy term added is that of a harmonic spring of the following form:

$$U_{c-s} = k \cdot r_{c-s}^2 \quad (2.3)$$

To coincide with the changes in the potential the values in Table 2.4 were used for the core and shell charges. For the Buckingham portion of the MA potential that remained after altering the coulombic term with the core-shell, the values in Table 2.5 were used.

Table 2.4: Core and Shell Charges

Atom	core(e)	shell(e)
<i>Ti</i>	2.196	-
<i>O</i>	0.500	-1.598

Table 2.5: Buckingham Potential Parameters

Ion pair (<i>ij</i>)	A_{ij} (eV)	ρ_{ij} (Å)	C_{ij} (eVÅ ⁶)
<i>Ti</i> – <i>Ti</i>	31120.528	0.154	5.25
<i>Ti</i> – <i>O</i>	16957.710	0.194	12.59
<i>O</i> – <i>O</i>	11782.884	0.234	30.22

Chapter 3

Simulations and Discussion

3.1 Validating the Model

By using the software package LAMMPS (Large-scale Atomic/Molecular Massively Parallel Simulator)[29], maintained by Sandia National Laboratories, MD simulations of titanate bulks and nanofibers can be run. However, building the simulation model and experiment must be carefully done as to avoid any simulation failures.

3.1.1 Building a Titanate Bulk

The first step in preparing a model for any kind of production simulation is to prepare a bulk simulation. This is intended to simulate a continuous infinite block of the material. Using this bulk will act like the control experiment for comparison with any future experiments using this material's model; it provides a ground state for the sample. The procedures for creating a bulk of rutile compared to anatase are similar and therefore only need to be described in a more general sense of creating a titanate bulk. For tetragonal crystals, this is a straight forward geometrical process; however, it causes the number of atoms in the unit cell to increase.

The initial step taken was to determine an orthogonal unit cell for the material.

This procedure was done as described in Section 2.1, by taking the known crystallographic structure and manipulating it such that an orthogonal cell could be drawn from it. Following the derivation of the position vectors of the atoms in an orthogonal cell, a single scaled unit cell was generated by multiplying the atoms' basis vector with the proper lattice constants. This unit cell was then replicated along the crystal's a , b , and c axis, to produce a functional simulation cell. The necessity to expand the bulk is based on the need to create enough space relative to the interatomic potential's cutoffs to ensure that no atom interacts with any duplicate atom. Briefly, the infinite bulk is modeled with a finite crystal in a simulation cell that has periodic boundary conditions. This means, e.g., the upper edge of the simulation box in any of the three dimensions, interacts through the upper bound with the atoms at the lower edge of the simulation cell in the given dimension. No atom can be permitted to interact with any in both directions along a dimension. Therefore, the minimum cell size is typically twice the longest interatomic cutoff distance. To confirm that the simulation cell is created properly a density profile of the atom's position such as Figure 3.1 and Figure 3.2 is generated to confirm that the cell is both large enough and that stoichiometry is maintained. Appendix A contains the generalized simulation bulk generated used for the purposes of this thesis.

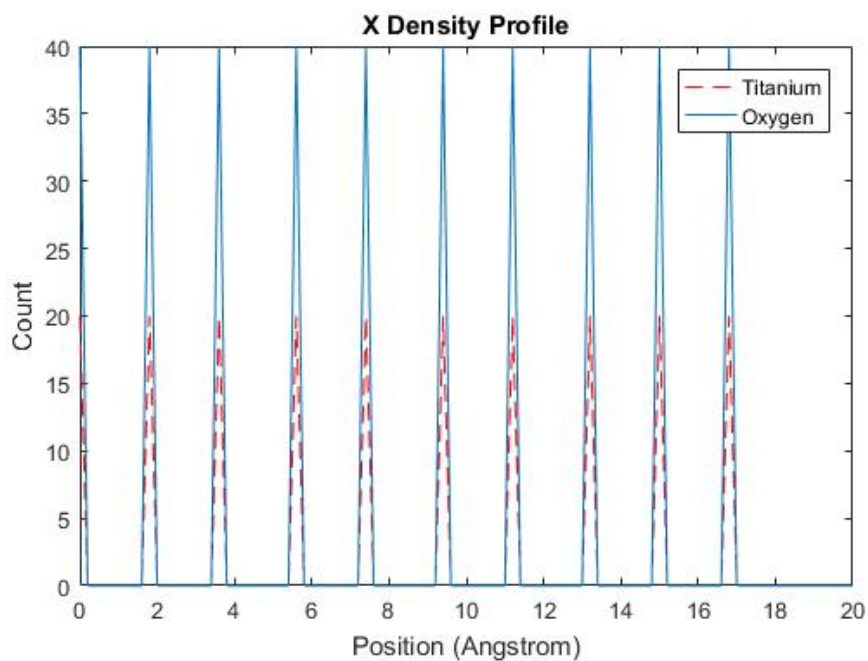


Figure 3.1: Density profile of anatase bulk along the X (a lattice) axis direction. This sample was about 20 Å on edge.

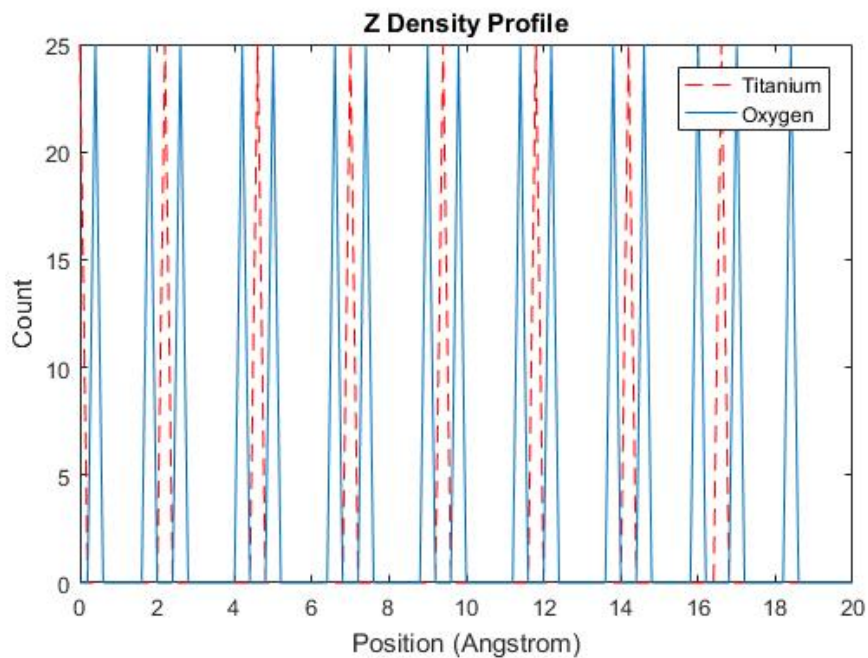


Figure 3.2: Density profile of anatase bulk along the Z (c lattice) axis direction. This sample was about 20 Å on edge.

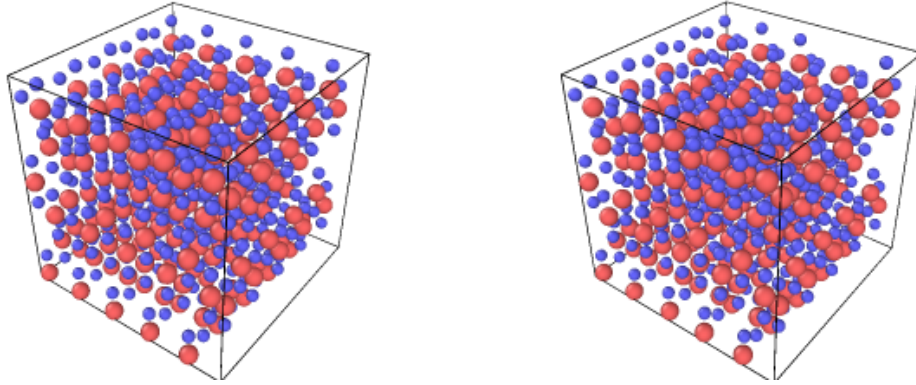


Figure 3.3: Atom positions before and after minimization runs of a 20 Å on edge bulk crystal.

3.1.2 Minimizing the Bulk Energy

After generating a proper bulk simulation cell, an energy minimization was performed on it. The reasoning behind this is that the newly generated cell has all its atoms position in the perfect crystalline location. This generates an energy imbalance as even at near 0K there are minor atomistic vibrations. To minimize the energy, a constant temperature and constant pressure simulation is run. To further drive that this simulation is a continuum of the desired material, the simulation cell is designated to have periodic boundary conditions on all three dimensions. This potential was generated with lattice constants at 300K, therefore, the energy minimization run in this system was run at the same temperature, the system was also held constant at 0 GPa. Figure 3.3 shows the before and after structures of a minimized anatase bulk.

This is a deviation on normal procedure as usually this is done by trying to drive the system's temperature to 0K. The reason behind this deviation is that due to the imparted core-shell particles in the simulation cell, without taking the energy data of the center of mass of the core-shell pair, the temperature in the system would not settle down to 0, instead the core-shell pairs would reside in another temperature even though the thermostat would claim the system has

reached the desired temperature. For the scope of this thesis, it was determined that to reduce the complexities of this process, it would be left for a future researcher to attempt the more complex routine to additionally confirm the validity of this model.

Running this simulation also confirms that the potential is a valid potential for this model. This is done by drawing comparisons to the observed lattice constants versus those derived from the simulation run, these comparisons can be seen in Table 3.1. The presented numbers from the simulation are satisfactory in comparison with the observed data for this material and therefore confirms that this bulk can be used to produce other experiments.

Table 3.1: Lattice values for titanate bulk structures

(a) Lattice comparison for Rutile

Direction	Expected	Calc
a-axis	4.594 Å	4.505 Å
c-axis	2.959 Å	3.016 Å

(b) Lattice comparison for Anatase

Direction	Expected	Calc
a-axis	3.776 Å	3.782 Å
c-axis	9.486 Å	9.570 Å

Following standard minimization preparing a slab to perform surface calculations requires another look at the density profile, it can be observed that to create a free surface slab that is oxygen terminated the final oxygen layer can be transferred to the bottom of the current bulk. This combined with the removal of periodic boundary conditions create a simulated infinite slab of the structure. Observing the density profile along the X (a) axis in Figure 3.1, a similar slab can be created by just removing periodicity as the layer repetitions are equal.

As this process of moving the layers of oxygen is done after an initial bulk

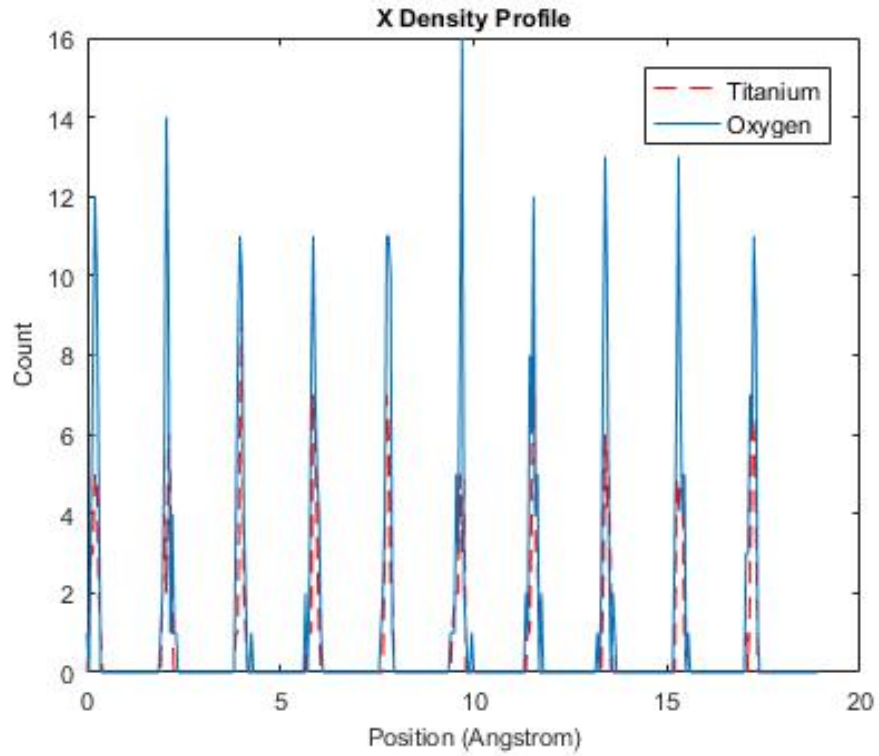


Figure 3.4: Density profile of anatase bulk along the X (a lattice) axis direction after minimization and shift. This sample was about 20 Å on edge.

minimization the atoms are no longer in their perfect position, therefore the profiles are not as sharp as those in the previously discussed figures, and after the transfer of the layers is completed by using a custom code the density profiles of the newly created slab samples are represented by Figure 3.4 and Figure 3.5.

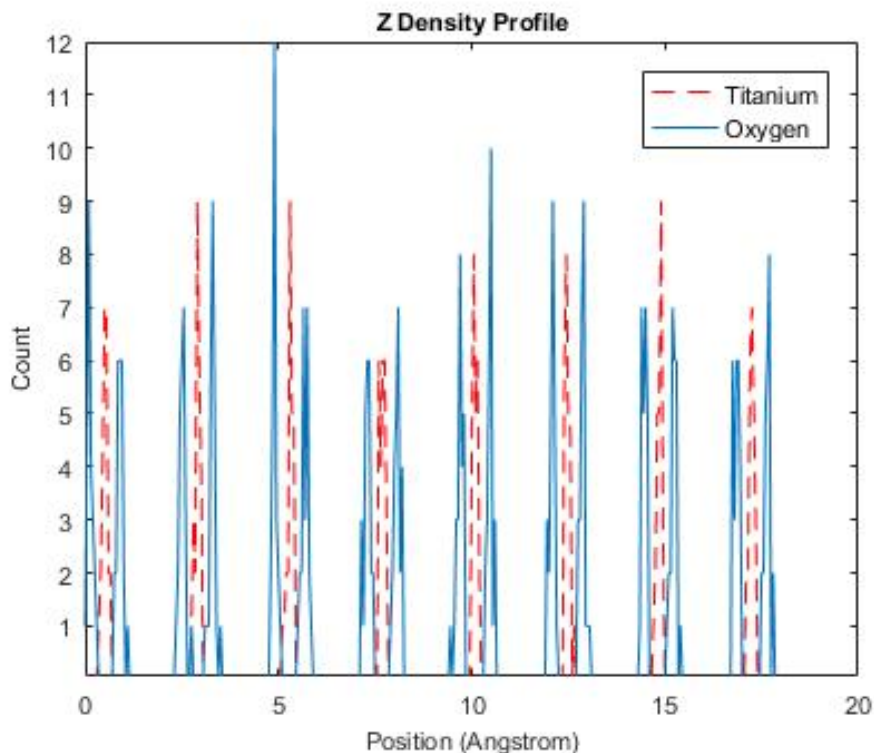


Figure 3.5: Density profile of anatase bulk along the Z (c lattice) axis direction after minimization and shift. This sample was about 20 Å on edge.

3.1.3 Simulating for Size Effects

Due to the long distance effect of the charges placed on the atoms in this simulation, one must be cautious to determine if there are interactions due to the sizing of the system. One way to determine if there is such a presence is to observe what the free surface energies of a simulated slab of material are and if they alter if the system gets larger or smaller. For this thesis, three slabs of anatase were used to observe the sizing effects: a 2 nm thick slab, a 4 nm thick slab, a 6 nm thick slab. These slabs were created following the procedure outlined in the previous subsection. Following the correct shifts in layers as seen by the density profiles, a slab simulation can be run using a canonical thermostat. These simulations allow the atoms to relax further and sometimes have free-surface reconstruct, although the latter is not the case here.

As seen by Figure 3.9 in the density profile or Figure 3.7 in the simulation

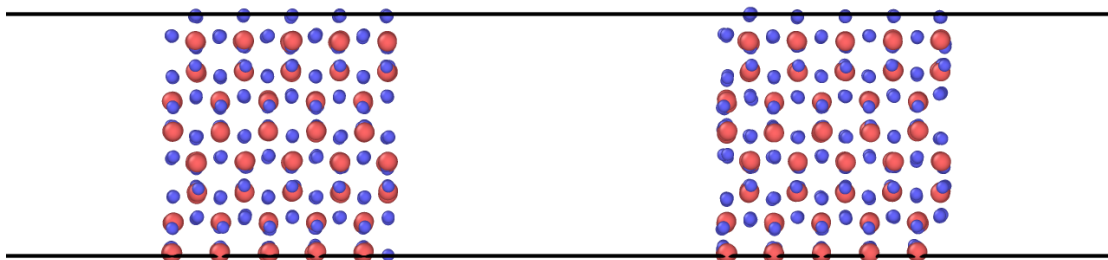


Figure 3.6: Anatase slab with periodicity removed in the X (a lattice) axis direction before and after relaxation. This sample was about 20 Å on edge.

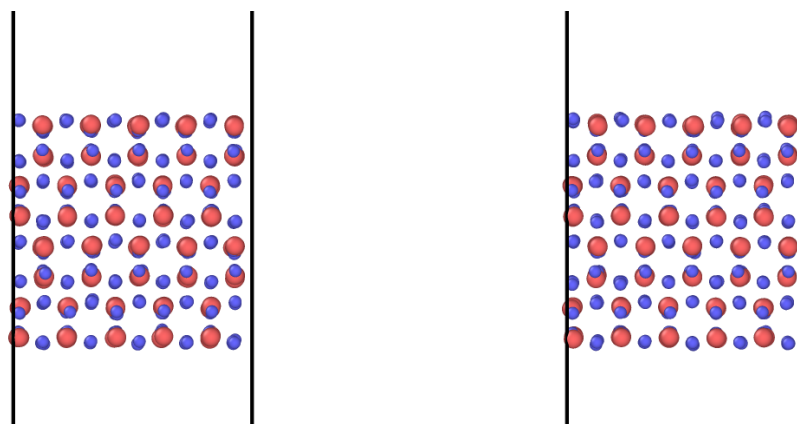


Figure 3.7: Anatase slab with periodicity removed in the Z (c lattice) axis direction before and after relaxation. This sample was about 20 Å on edge.

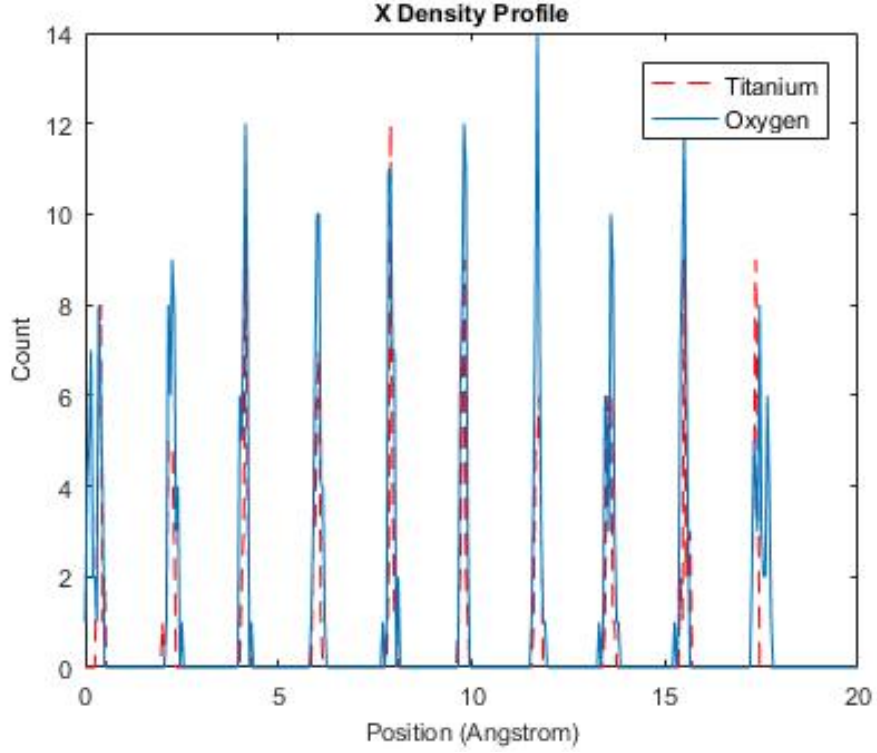


Figure 3.8: Density profile of anatase bulk along the X (a lattice) axis direction after relaxation. This sample was about 20 Å on edge.

before and after, if the free surface normal to the c-axis is run with the proper layering of the crystal, the oxygen atoms seem to relax a small amount more but there is no significant change in structure. However, as seen by Figure 3.9 or Figure 3.6 in the simulation, if the free surface is normal to the a-axis, the oxygen atoms relax away from remaining in the same plane as the titanium atoms. This is a well observed phenomena in metallic oxide systems, and has been documented by *S.Blonski and S.H.Garofalini* [30].

Using the total energy of the bulk compared to that of the slab and slab's surface area, A , the surface energy can be calculated using the following formula:

$$E_{surface} = \frac{E_{slab} - E_{bulk}}{2(L_x L_y)} \quad (3.1)$$

Table 3.2 tabulates the data observed from these simulations, which concluded in that there are noticeable size effects with this model within this small length

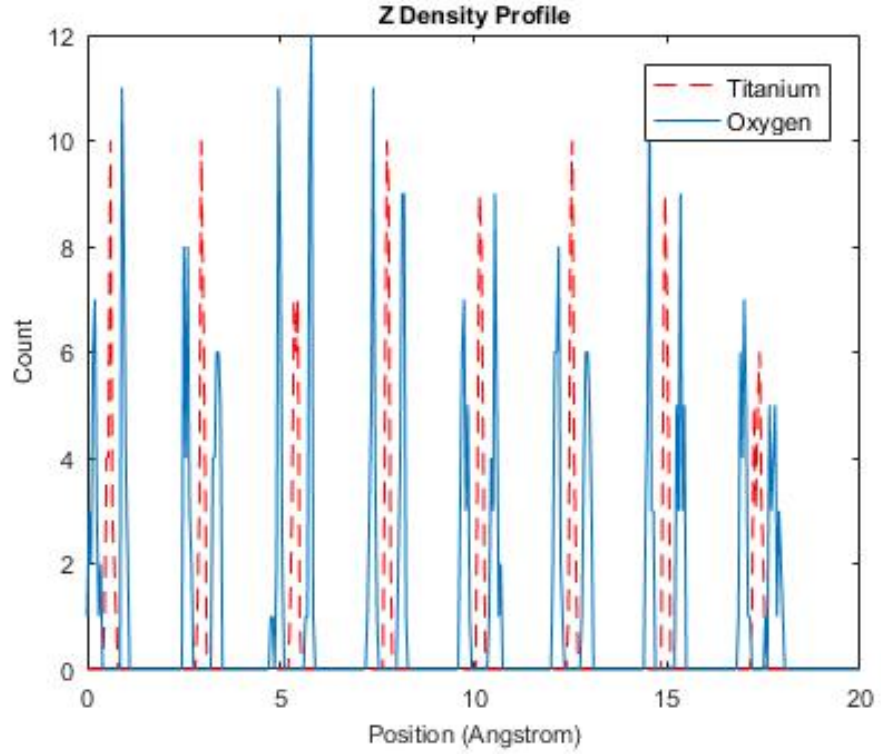


Figure 3.9: Density profile of anatase bulk along the Z (c lattice) axis direction after relaxation. This sample was about 20 Å on edge.

scale.

Table 3.2: Surface Energies of Slab versus Slab Size

Size	c-axis Energy (eV/Å ²)	a-axis Energy (eV/Å ²)
20Å	0.9700	0.1063
40Å	0.0887	0.1010
60Å	0.0812	0.0976

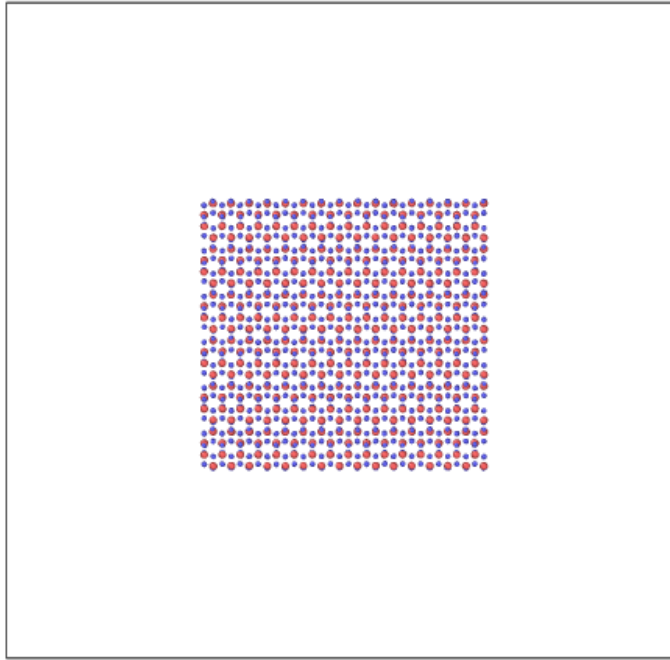


Figure 3.10: Simulation cell of anatase nanowire at the initial simulation timestep.

3.2 Nanowire Simulation

Using the starting point of a slab that has not been relaxed similar to the one from Section 3.1.3, a nanowire can be formed by removing the periodicity in a second direction. In this thesis, periodicity was removed by expanding the bounding box to be greater than the size of the lattice being simulated in the c and b lattice axis directions (X and Y) while maintaining periodicity in the a lattice axis direction (X), therefore creating two free surfaces. This was done to the slab of 6 nm thickness to create a wire that had a 6 nm by 6 nm square cross section of "infinite" length (due to periodic boundary conditions; the actual extent of the system along X is about 6 nm). Figure 3.10 shows the bounding box with the simulated wire section before running the minimization. Figure 3.11 then shows the final temp step result of the minimization.

At first glance, the final time-step is a far deviation from the initial time-step. However, it is imperative to remember what methods were applied to create this

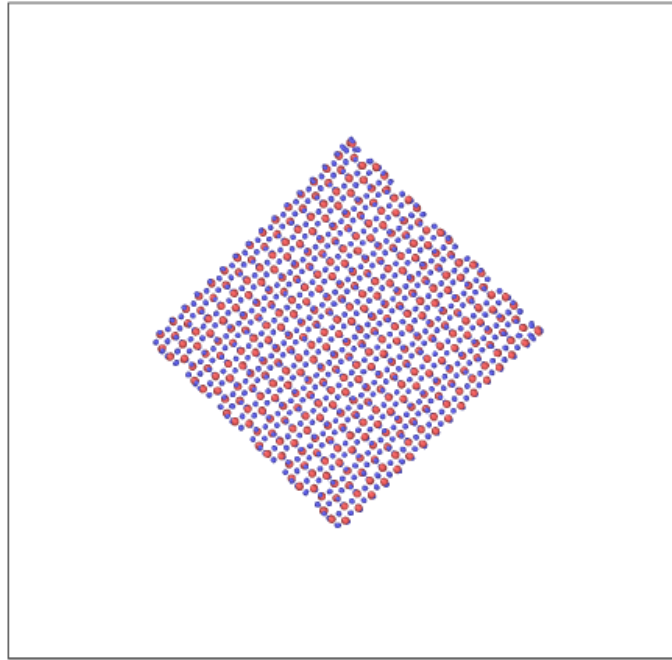


Figure 3.11: Simulation cell of anatase nanowire at the final simulation timestep.

simulation, primarily the boundary conditions. The method in which periodicity was thought to be removed was by making the bounding box larger as to mitigate any long-range effects the model's potential would have. This method, however, would really create a virtual array of nanowire, such as Figure 3.13. This array would then be constructed from several copies of one parent nanowire as it was simulated. Therefore, when running a simulation of this nanowire, initially, it is witnessed to have the oxygen in the layers of oxygen and titanium shift slightly towards the surface as predicted by slab simulation in the previous section. This makes it so that all of the outer surfaces of the each individual nanowire is a layer of oxygen, which carries a negative charge atomic charge. Since all the nanowires in this array are from the same parent nanowire, all of the nanowires now also have negative oxygen atoms at their surfaces, therefore, if the wires are in close enough proximity to each other the negative side would repel like magnets and attempt to find a state of lowest energy. In the case of this simulation, the nanowire array

preceded to interact as such and therefore cause each wire to rotate from their starting configuration to a configuration where the closest points between each nanowire was the corner point of each structure minimizing the force at which these wire are repelling each other. Furthermore, there is the implication of how this could affect the overall energy of the system as there exist long range interactions. Shown in Figure 3.12, the potential energy of the system is steady around the full time average of the potential energy until just before timestep 8500, or 8.5ps. At this point the system becomes unsettled and rotates to the new position and begins to settle down again around timestep 140000, 14 ps. The system returns to be stable with energy fluctuating around the time average potential energy for the remaining 6 ps of the simulation. In this case, this process has contributed a small amount of energy but even at this scale can be said was of negligible effect to the results as the energy of the system was only effected by .009% of the total potential energy prior to rotation compared to that of the total potential energy post-rotation. That such a small energy difference drives the significant rotation observed seems curious but it is also of note that the slave has zero resistance to rotation about that axis.

Due to the interaction the long-range terms of the other virtual nanowires it is not safe to assume that this nanowire is isolated and can have proprieties derived as such. Any properties that were to be derived from this simulation would be a set of properties generated for an array of wires and not a singular wire. As such, there can be a study of the calculated formation energies of this nanowire array based off the final energy of this system, the energy of the bulk, and the number of stoichiometric units using the following equation:

$$E_{formation} = \frac{E_{nanowires} - E_{bulk}}{N} \quad (3.2)$$

Where $E_{formation}$ is the formation energy of a nanowire array, $E_{nanowire}$ is the

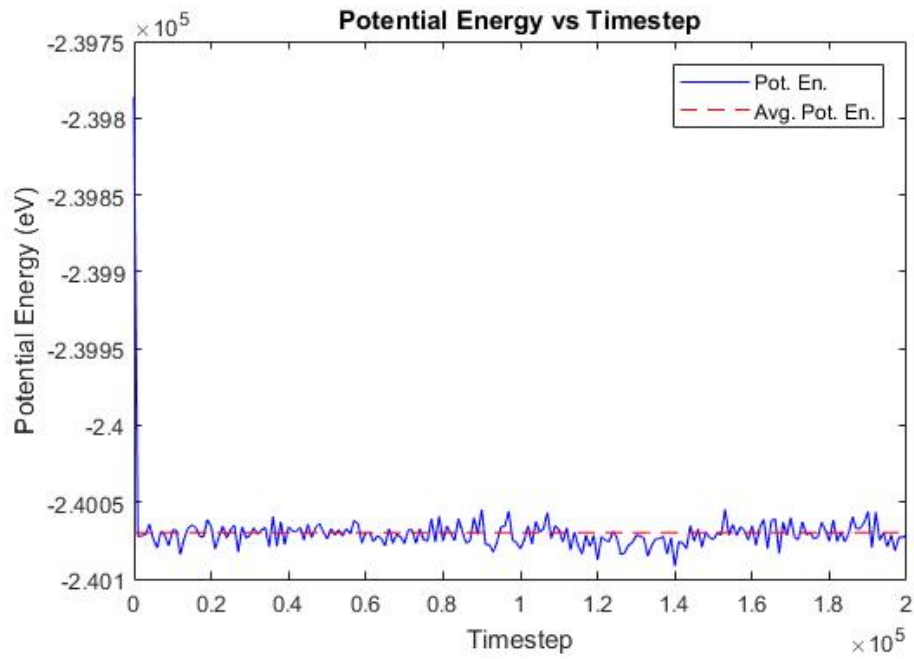


Figure 3.12: Potential energy of nanowire simulation with respect to time.

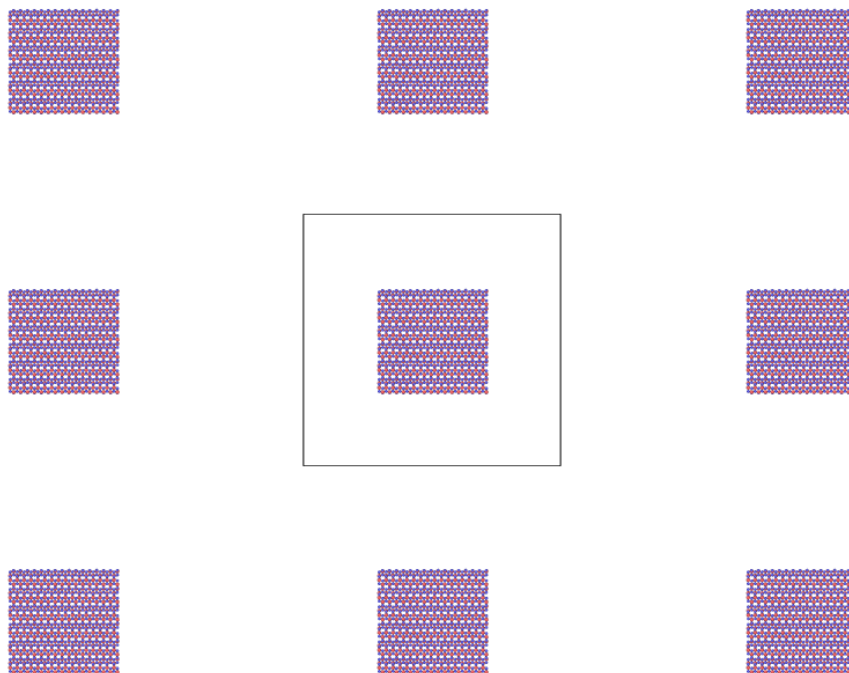


Figure 3.13: Image of simulated anatase nanowire array at the initial simulation timestep. Only the center set of atoms were simulated (inside bounding box), all others are a representation of the nanowires surrounding the center.

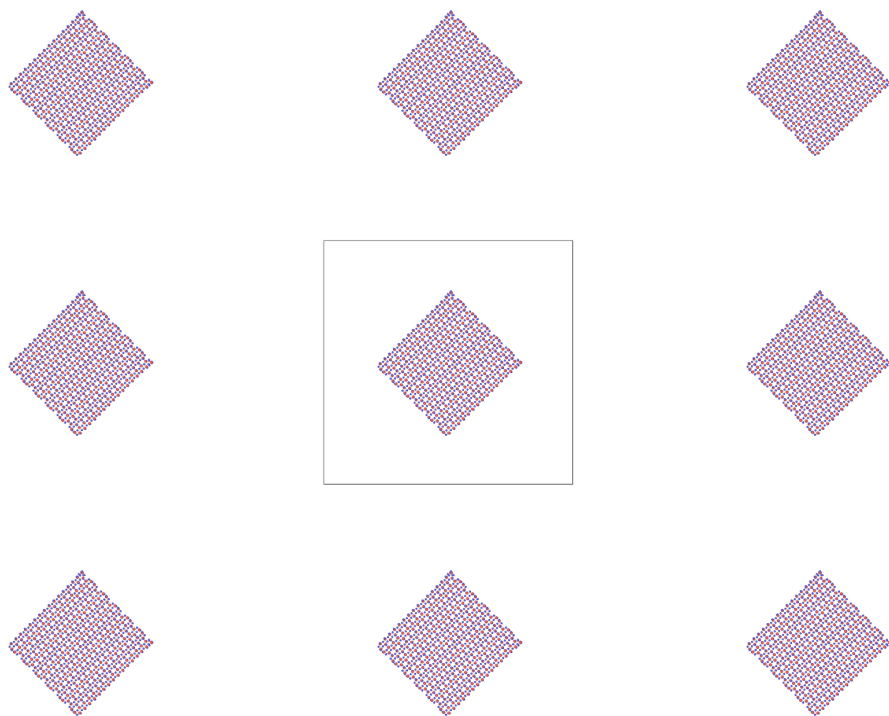


Figure 3.14: Image of simulated anatase nanowire array at the final simulation timestep. Only the center set of atoms were simulated (inside bounding box), all others are a representation of the nanowires surrounding the center.

final potential energy of the nanowire, E_{slab} is the final potential energy of the "infinite" bulk, and N is the number of stoichiometric units. Thus, it is calculated that the enthalpy of formation of these nanowires relative to a TiO_2 bulk is 19.958 kJ/mol (4.77 kcal/mol) in this simulation. Comparing this result relative with the known standard enthalpy of formation for a titanium oxide bulk solid of 945 kJ/mol , this energy is reasonable as there would be an energy cost compared to the formation of the bulk to form the two free-surface directions present in the titanate nanowire.

Chapter 4

Future Work

The scope of this thesis was limited in the realm of establishing the foundation for future research to be conducted by a doctoral candidate. Thus, this thesis accomplished the following goals:

- Validated the usage of the potential model set forth by *Kerisit et. al.*
- Established that a closer look is needed at the size effects of the potential and that simulation may have to be carried out in a different manner than those conducted in this thesis.

As observed by the Section 3.1, the potential model is of use to analyze titanates. The finding here dictate that although more simulation samples are required to establish a tolerance of the results, that the initial results are promising for full implementation of the model. Additionally, the potential model offers integration of lithium into the titanate structure for charge transfer analysis which is not covered within the scope of this thesis and is a future research goal for a future researcher. Also not covered within the scope of this project is the formation of unique layered titanate systems that could have this long range potential model applied.

Established also in Section 3.1.3 is that there are definite effects on the size of the system being simulated. The smaller the simulated slab or wire, the more internal effects of the charges on atoms there are on the surface energies. Thus a study must be conducted further in which how the effects progress as the system grows larger. These sizing effects could have different effects on the simulated mechanical proprieties of the nanowire, such as the tensile strength.

Section 3.2 attempted to simulate an isolated nanowire, however, due to the long-range effects of this potential, there is interaction among other virtual nanowires in the system. This led to the inability to perform calculations to derive individual material properties from the simulation. Therefore, due to the time constraints of this thesis, future research will have to further study the isolated nanowire instead of one that has been affected by an array of such. These studies will further both the knowledge of the potential and create a foundation for attempts into simulating lithium interactions in the nanowire.

Bibliography

- [1] Omar Ellabban, Haitham Abu-Rub, and Frede Blaabjerg. “Renewable energy resources: Current status, future prospects and their enabling technology”. In: *Renewable and Sustainable Energy Reviews* 39 (2014), pp. 748–764. ISSN: 1364-0321. DOI: <http://dx.doi.org/10.1016/j.rser.2014.07.113>. URL: <http://www.sciencedirect.com/science/article/pii/S1364032114005656>.
- [2] Ibrahim Dincer. “Renewable energy and sustainable development: a crucial review”. In: *Renewable and Sustainable Energy Reviews* 4.2 (2000), pp. 157–175. ISSN: 1364-0321. DOI: [http://dx.doi.org/10.1016/S1364-0321\(99\)00011-8](http://dx.doi.org/10.1016/S1364-0321(99)00011-8). URL: <http://www.sciencedirect.com/science/article/pii/S1364032199000118>.
- [3] Jitendra N. Tiwari, Rajanish N. Tiwari, and Kwang S. Kim. “Zero-dimensional, one-dimensional, two-dimensional and three-dimensional nanostructured materials for advanced electrochemical energy devices”. In: *Progress in Materials Science* 57.4 (2012), pp. 724–803. ISSN: 00796425. DOI: 10.1016/j.pmatsci.2011.08.003. URL: <http://dx.doi.org/10.1016/j.pmatsci.2011.08.003>.
- [4] Sheneve Z. Butler et al. “Progress, Challenges, and Opportunities in Two-Dimensional Materials Beyond Graphene”. In: *ACS Nano* 7.4 (2013). PMID: 23464873, pp. 2898–2926. DOI: 10.1021/n400280c. eprint: <http://dx.doi.org/10.1021/n400280c>. URL: <http://dx.doi.org/10.1021/n400280c>.

- [5] Matthias Karg et al. “Atomic Layer Deposition of Silica on Carbon Nanotubes”. In: *Chemistry of Materials* 29.11 (2017), pp. 4920–4931. DOI: 10.1021/acs.chemmater.7b01165. eprint: <http://dx.doi.org/10.1021/acs.chemmater.7b01165>. URL: <http://dx.doi.org/10.1021/acs.chemmater.7b01165>.
- [6] Feng Lin, Y. Xiang, and Hui-Shen Shen. “Temperature dependent mechanical properties of graphene reinforced polymer nanocomposites – A molecular dynamics simulation”. In: *Composites Part B: Engineering* 111 (2017), pp. 261–269. ISSN: 1359-8368. DOI: <http://dx.doi.org/10.1016/j.compositesb.2016.12.004>. URL: <http://www.sciencedirect.com/science/article/pii/S135983681632203X>.
- [7] Yan B. Vogel et al. “Hydrogen evolution during the electrodeposition of gold nanoparticles at Si(100) photoelectrodes impairs the analysis of current-time transients”. In: *Electrochimica Acta* 247 (2017), pp. 200–206. ISSN: 0013-4686. DOI: <http://dx.doi.org/10.1016/j.electacta.2017.06.126>. URL: <http://www.sciencedirect.com/science/article/pii/S0013468617313646>.
- [8] Pradip Kr. Ghorai and Sharon C. Glotzer. “Molecular Dynamics Simulation Study of Self-Assembled Monolayers of Alkanethiol Surfactants on Spherical Gold Nanoparticles”. In: *The Journal of Physical Chemistry C* 111.43 (2007), pp. 15857–15862. DOI: 10.1021/jp0746289. eprint: <http://dx.doi.org/10.1021/jp0746289>. URL: <http://dx.doi.org/10.1021/jp0746289>.
- [9] Shin-Pon Ju, Jenn-Sen Lin, and Wen-Jay Lee. “A molecular dynamics study of the tensile behaviour of ultrathin gold nanowires”. In: *Nanotechnology* 15.9 (2004), p. 1221.
- [10] Yeau-Ren Jeng, Ping-Chi Tsai, and Te-Hua Fang. “Molecular dynamics investigation of the mechanical properties of gallium nitride nanotubes under tension and fatigue”. In: *Nanotechnology* 15.12 (2004), p. 1737.

- [11] Zhong-Yong Yuan and Bao-Lian Su. “Titanium oxide nanotubes, nanofibers and nanowires”. In: *Colloids and Surfaces A: Physicochemical and Engineering Aspects* 241.1 (2004), pp. 173–183. ISSN: 09277757. DOI: 10.1016/j.colsurfa.2004.04.030.
- [12] Sung Kyu Choi et al. “Photocatalytic comparison of TiO₂ nanoparticles and electrospun TiO₂ nanofibers: Effects of mesoporosity and interparticle charge transfer”. In: *Journal of Physical Chemistry C* 114.39 (2010), pp. 16475–16480. DOI: 10.1021/jp104317x.
- [13] Ulrike Diebold. “The surface science of titanium dioxide”. In: *Surface Science Reports* 48.5 (2003), pp. 53–229. ISSN: 0167-5729. DOI: [http://dx.doi.org/10.1016/S0167-5729\(02\)00100-0](http://dx.doi.org/10.1016/S0167-5729(02)00100-0). URL: <http://www.sciencedirect.com/science/article/pii/S0167572902001000>.
- [14] Larry L Hench and Jon K West. “The sol-gel process”. In: *Chemical reviews* 90.1 (1990), pp. 33–72.
- [15] Yassine Bessekhoud, Didier Robert, and Jean Victor Weber. “Synthesis of photocatalytic TiO₂ nanoparticles: optimization of the preparation conditions”. In: *Journal of Photochemistry and Photobiology A: Chemistry* 157.1 (2003), pp. 47–53. ISSN: 1010-6030. DOI: [http://dx.doi.org/10.1016/S1010-6030\(03\)00077-7](http://dx.doi.org/10.1016/S1010-6030(03)00077-7). URL: <http://www.sciencedirect.com/science/article/pii/S1010603003000777>.
- [16] A. Kundu. *Rapid synthesis of titanate nanomaterials*. US Patent App. 12/138,928. May 2009. URL: <https://www.google.com/patents/US20090117028>.
- [17] Dan Behnke. *Anatase crystal, 1 mm tall*. University of Wisconsin System. URL: <https://wgnhs.uwex.edu/minerals/anatase/>.
- [18] G. V. Samsonov. *The Oxide Handbook*. Springer Verlag, 2012.

- [19] Nick Greeves. *ChemTube3D*. 2017. URL: <http://www.chemtube3d.com/index.html>.
- [20] Aneesur Rahman and Frank H. Stillinger. “Molecular Dynamics Study of Liquid Water”. In: *The Journal of Chemical Physics* 55.7 (1971), pp. 3336–3359. DOI: 10.1063/1.1676585. eprint: <http://dx.doi.org/10.1063/1.1676585>. URL: <http://dx.doi.org/10.1063/1.1676585>.
- [21] Aaron Oaks. *Development of Generalized KMC Code to Study Defect Mobility in Ceramic Materials towards Nuclear Fuel Applications*. May 2010.
- [22] Kai Kadau, Timothy C Germann, and Peter S Lomdahl. “Molecular dynamics comes of age: 320 billion atom simulation on BlueGene/L”. In: *International Journal of Modern Physics C* 17.12 (2006), pp. 1755–1761.
- [23] Daan Frenkel and Berend Smit. *Understanding molecular simulation: from algorithms to applications*. Vol. 1. Academic press, 2001.
- [24] Richard LeSar. *Introduction to computational materials science: fundamentals to applications*. Cambridge University Press, 2013.
- [25] J. E. Jones. “On the Determination of Molecular Fields. II. From the Equation of State of a Gas”. In: *Proceedings of the Royal Society of London A: Mathematical, Physical and Engineering Sciences* 106.738 (1924), pp. 463–477. ISSN: 0950-1207. DOI: 10.1098/rspa.1924.0082. eprint: <http://rspa.royalsocietypublishing.org/content/106/738/463.full.pdf>. URL: <http://rspa.royalsocietypublishing.org/content/106/738/463>.
- [26] R. A. Buckingham. “The Classical Equation of State of Gaseous Helium, Neon and Argon”. In: *Proceedings of the Royal Society of London A: Mathematical, Physical and Engineering Sciences* 168.933 (1938), pp. 264–283. ISSN: 0080-4630. DOI: 10.1098/rspa.1938.0173. eprint: <http://rspa.royalsocietypublishing.org/content/168/933/264.full.pdf>. URL: <http://rspa.royalsocietypublishing.org/content/168/933/264>.

- [27] Masanori Matsui and Masaki Akaogi. “Molecular dynamics simulation of the structural and physical properties of the four polymorphs of TiO₂”. In: *Molecular Simulation* 6.4-6 (1991), pp. 239–244.
- [28] Sebastien Kerisit et al. “A Shell Model for Atomistic Simulation of Charge Transfer in Titania”. In: *The Journal of Physical Chemistry C* 112.20 (2008), pp. 7678–7688. DOI: 10.1021/jp8007865.
- [29] Steve Plimpton. “Fast Parallel Algorithms for Short-Range Molecular Dynamics”. In: *Journal of Computational Physics* 117.1 (1995), pp. 1–19. ISSN: 0021-9991. DOI: <http://dx.doi.org/10.1006/jcph.1995.1039>. URL: <http://www.sciencedirect.com/science/article/pii/S002199918571039X>.
- [30] S. Blonski and S.H. Garofalini. “Molecular dynamics simulations of α -alumina and γ -alumina surfaces”. In: *Surface Science* 295.1 (1993), pp. 263–274. ISSN: 0039-6028. DOI: [http://dx.doi.org/10.1016/0039-6028\(93\)90202-U](http://dx.doi.org/10.1016/0039-6028(93)90202-U). URL: <http://www.sciencedirect.com/science/article/pii/003960289390202U>.

Biography

Nicholas Lima Acosta was born in São Paulo, SP, Brazil to Luis and Karla Acosta. Nick immigrated to the United States and grew up in Westampton, New Jersey and attended the Burlington County Institute of Technology - Westampton Campus where he graduated with honors in 2011. Following his successes in high school, Nick enrolled at Lehigh University in Bethlehem, PA and graduated in 2015 with a Bachelor of Science in Mechanical Engineering. He then continued on the graduate program at Lehigh for his Masters degree the following semester.

During his time at Lehigh, Nick was continuously involved in activities, both in and out of Lehigh. He was part of the Lehigh Formula SAE team for his 4 years as an undergraduate student, spending his final two years with the team as the lead chassis designer. Nick also was the lead sound engineer and designer for the Lehigh Mustard & Cheese Drama Society's presentation of Reefer Madness. Out of Lehigh, Nick was involved in the community as a volunteer mentor for FIRST Robotics teams in the region. This volunteer experience combined with his involvement in being a teaching assistant at Lehigh for ME 121, Mechanical Engineering Lab II, and ME 240, Manufacturing, grew his passion for teaching, particularly younger students. Upon completion of his Master's from Lehigh, Nick will be following his passion for teaching by joining the faculty of Burlington County Institute of Technology - Westampton Campus as the instructor for Pre-Engineering and technical mentor for FIRST Robotics Team 816.